

# A universal scaling law of black hole activity including gamma-ray bursts

F. Y. Wang<sup>1,2★</sup> & Z. G. Dai<sup>1,2</sup>

<sup>1</sup>*School of Astronomy and Space Science, Nanjing University, Nanjing 210093, China*

<sup>2</sup>*Key Laboratory of Modern Astronomy and Astrophysics (Nanjing University), Ministry of Education, Nanjing 210093, China*

## ABSTRACT

Previous works show that a correlation among radio luminosity, X-ray luminosity, and black hole (BH) mass from stellar-mass BHs in X-ray binaries to supermassive BHs in active galactic nuclei (AGNs), which leads to the so-called fundamental plane of BH activity. However, there are two competing explanations for this fundamental plane, including the jet-dominated model and the disk-jet model. Thus, the physical origin of this fundamental plane remains unknown. In this paper, we show that the X-ray luminosities, radio luminosities and BH masses of gamma-ray bursts (GRBs) and M82 X-1 also show a similar distribution. The universal scaling law among stellar-mass, intermediate and supermassive BH systems, together with the fact that radio and X-ray emission of GRBs originates from relativistic jets, reveals that the fundamental plane of BH activity is controlled by a jet, i.e., the radio and X-ray emission is mainly from the jet. Our work also suggests that the jets are scale-invariant with respect to the BH mass.

**Key words:** gamma-ray burst: general – radiation mechanism: non-thermal

## 1 INTRODUCTION

A long-standing and intriguing question is that the similarity among stellar, intermediate and supermassive black holes (BHs) and their relativistic jets (White et al. 1984; Mirabel & Rodriguez 1999; Meier 2003). Some interesting results have been found, including the similar accretion pro-

★ E-mail: fayinwang@nju.edu.cn

cess (McHardy et al. 2006), radiation mechanism (Wang et al. 2014), statistical properties of X-ray flares (Wang et al. 2015) and energetics of relativistic jets (Nemmen et al. 2012).

A tight correlation between the radio luminosity and X-ray luminosity has been firstly discovered in X-ray binaries GX 339-4 and V404 Cyg (Corbel et al. 2000; Gallo et al. 2003). After considering the BH mass, AGNs show a similar correlation, which is called the fundamental plane of BH activity (Merloni et al. 2003; Falcke et al. 2004). This correlation has been confirmed by later studies (Körding et al. 2006; Li et al. 2008; Yuan et al. 2009; Gültekin et al. 2014). Lü et al. (2015) showed that radio luminosity correlated with X-ray luminosity for gamma-ray bursts (GRBs). However, the power-law slope is slightly different with the one found in X-ray binaries (Corbel et al. 2000; Gallo et al. 2003). Although some doubts on the existence of the fundamental plane have been raised, Merloni et al. (2006) presented that the fundamental plane correlation cannot be a distance artifact, and that it must represent the intrinsic characteristic of BHs. The fundamental plane attempts to unify sources associated with BHs, over a large range of masses and luminosities, from Galactic sources to AGNs. However, some XRBs might not follow the fundamental plane (Corbel et al. 2004). Some other outliers have been found (Jonker et al. 2010; Coriat et al. 2011; Ratti et al. 2012). For the sub-Eddington objects, i.e., low/hard state of XRBs and low-luminosity AGNs, Körding et al. (2006) found that the fundamental plane is much tighter than the full sample. Therefore, they concluded that the fundamental plane should be most suitable for radiatively inefficient BH sources. Another form of the fundamental plane for radiatively efficient BHs is established by Dong et al. (2014) and Xie & Yuan (2017).

However, the physical origin of the fundamental plane and its relationship with the physical properties of the sources are mysterious (Narayan 2005). There are at least two possible explanations for the origin of the fundamental plane. The first explanation is that the radio and X-ray emission for BH sources is attributed to synchrotron emission from a jet in the jet-dominated state. Because the radio and X-rays emission is powered by the jet, a tight correlation between them could be expected (Falcke et al. 2004; Yuan & Cui 2005). For example, Markoff et al. (2003) modeled the broadband spectrum of X-ray binary GX 339-4 and explained the fundamental plane using the jet model. Although, the disk component may contribute  $\leq 20$  per cent in the soft X-ray band for low/hard state of some black hole X-ray binaries (Poutanen 1998; Fender 2001; Markoff & Nowak 2004; Homan et al. 2005; Markoff et al. 2005; Remillard & McClintock 2006). On the other hand, the X-ray emission may originate from the accretion flow, while the radio emission is produced by the relativistic jet. Meanwhile, the accretion flow and the jet are strongly coupled, so that the radio and X-ray luminosity is correlated (Merloni et al. 2003; Heinz & Sunyaev

2003). When the X-ray luminosity is below a critical value, the X-ray radiation should be dominated by emission from the jet rather than from the accretion flow (Yuan & Cui 2005). Yuan et al. (2009) showed that the X-ray emissions from IC 1459, M32, M81, M84, M87, NGC 3998, NGC 4594, NGC 4621, and NGC 4697 are jet-dominated. Younes et al. (2012) fitted the spectral energy distributions of six LINERs, and showed that the X-ray emission is jet-dominated. Hence, a further clarification is urgently needed. Moreover, whether intermediate-mass BHs follow this correlation remains unknown. Some candidates of intermediate-mass BHs have been found, such as M82 X-1 (Pasham et al. 2014), and HLX-1 (Farrell et al. 2009).

Gamma-ray bursts (GRBs) are the most powerful electromagnetic explosions in the universe. The progenitors of GRBs are thought to be massive stars (Woosley 1993) or mergers of compact stars (Eichler et al. 1989; Nakar 2007). So the central engine of GRBs may be stellar-mass BHs. The radiation in X-ray and radio bands is well understood, which originates from relativistic jets (Zhang & Mészáros 2004; Piran 2004; Mészáros 2006; Gehrels et al. 2009; Kumar & Zhang 2015). GRBs, as bright lighthouses in the distant universe, are ideal tools to probe the properties of the early universe (Wang et al. 2015). There are some similar properties between GRBs and AGNs, such as the variability property (Wu et al. 2016), and radiation mechanism (Lyu et al. 2014). However, whether GRBs follow the fundamental plane is unknown.

In this paper, we investigate the fundamental plane of BH activity including GRBs and the intermediate-mass BH M82 X-1. This paper is organized as follows. In Section 2, we present the sample of GRBs. The fitting results are presented in Section 3. Section 4 gives summary.

## 2 SAMPLES

We collect the data of GRBs from previous literature. Because the luminosity of GRBs is required, the GRBs with redshift measurements are selected. Meanwhile, the radio and X-ray observations are also required. There are 31 GRBs in our sample, which are listed in Table 1. In this table, columns 2 is the redshift of a GRB. The prompt emission flux measured between energy range of columns 5 and 6 is listed in columns 3. The peak energy  $E_{\text{peak}}$  of the spectrum is in columns 4. The low-energy and high-energy power-law spectral indices  $\alpha$  and  $\beta$  are given in columns 7 and 8, respectively. When the values of  $\alpha$  and  $\beta$  are unknown, the typical values  $\alpha = 1.1 \pm 0.4$  and  $\beta = 2.2 \pm 0.4$  are adopted (Schaefer 2007). The radio flux at observed frequency (column 10) is presented in Column 9. Column 11 is the references of parameters. For the radio flux, we use the peak radio flux from Chandra & Frail (2012). The isotropic radio luminosity at 5 GHz is calculated

by (Chandra & Frail 2012)

$$L_R = 4\pi d_L^2 \nu F_R F_{\text{beam}} (1+z)^{-\alpha_1-1}, \quad (1)$$

where  $d_L$  is the luminosity distance,  $F_R$  is radio flux at 5 GHz, and  $\alpha_1 = 1/3$  is the spectral slope in the slow cooling regime (Sari et al. 1998). The collimation-corrected luminosity is given by  $L_{R,c} = L_R F_{\text{beam}}$ , where  $F_{\text{beam}} = 1 - \cos \theta_j$  is the beaming factor, and the jet opening angle  $\theta_j$  is adopted from Wang et al. (2014). The observed radio flux is converted to the flux at 5 GHz using spectral slope  $\alpha_1 = 1/3$ . Because the X-ray flux declines quickly after the prompt emission, we adopt the X-ray flux at the prompt emission as an approximation of the peak value. The X-ray luminosity in 2 – 10 keV is  $L = 4\pi d_L^2 P_{\text{bolo}} F_{\text{beam}}$ , where  $P_{\text{bolo}}$  can be derived by

$$P_{\text{bolo}} = P \times \frac{\int_{2/(1+z)}^{10/(1+z)} E \Phi(E) dE}{\int_{E_{\min}}^{E_{\max}} E \Phi(E) dE}, \quad (2)$$

where  $P$  in units of  $\text{erg cm}^{-2} \text{s}^{-1}$  is the observed peak flux between  $E_{\min}$  and  $E_{\max}$ , and  $\Phi(E)$  is the Band function (Band et al. 1993). If the flux  $P$  is in units of  $\text{photons cm}^{-2} \text{s}^{-1}$ , the  $P_{\text{bolo}}$  is

$$P_{\text{bolo}} = P \times \frac{\int_{2/(1+z)}^{10/(1+z)} E \Phi(E) dE}{\int_{E_{\min}}^{E_{\max}} \Phi(E) dE}. \quad (3)$$

The mass of a GRB progenitor is still uncertain. The theoretical model of long GRBs is thought to be collapse of a massive star to a stellar-mass BH (Woosley 1993). While mergers of neutron star-neutron star or neutron star-BH binaries may produce short GRBs. So we adopt two assumptions for the mass,  $3M_{\odot}$  and  $10M_{\odot}$ , and 10% relative uncertainties. These values are consistent with numerical simulations (MacFadyen & Woosley 1999; Dessart et al. 2012).

Generally, the X-ray emission of GRB prompt emission is from internal shock, which is formed by collisions of relativistic shells (Rees & Mészáros 1994). After collisions, the shells will combine to one shell. This shell sweeps the external medium and produces the external shock. The radio emission of GRBs is from external shock, which is generated by the relativistic shell from central engine sweeping the external medium (Sari et al. 1998). So this jet must carry the memory of the central engine. It is reasonable to make an analogy between AGN and GRBs. For example, Nemmen et al. (2012) showed that jets produced by AGNs and GRBs exhibit the same correlation between the kinetic power and the gamma-ray luminosity.

For the X-ray binary (XRB) and AGN sample, we use the sample from Körding et al. (2006). This sample includes XRBs in the low/hard state. There are also low-luminosity AGN (LLAGN), LINERs (low ionization nuclear emission region), FR I Radio Galaxies and BL Lac objects in this sample. The masses of supermassive BHs are from  $10^7 M_{\odot}$  to  $10^9 M_{\odot}$ . Because of the existence

of different accretion states for XRBs, appropriate sources must be selected when studying the fundamental plane (Yuan & Cui 2005; Ho 2005; K rding 2014). Radio observations confirmed that the low/hard state is associated with a jet (Fender 2001). Different states of XRBs may follow different radio-X-ray correlations (Yuan & Cui 2005; K rding et al. 2006). We include GX 339-4 with  $8.0 \pm 2.0 M_{\odot}$  (K rding et al. 2006), V404 Cyg with  $12.0 \pm 2.5 M_{\odot}$  (K rding et al. 2006), 4U 1543-475 with  $9.4 \pm 1.0 M_{\odot}$  (Remillard & McClintock 2006), and XTE 1118+480 with  $6.8 \pm 0.5 M_{\odot}$  (Remillard & McClintock 2006). For Sgr A\*, we include the hard X-ray flare observed by Baganoff et al. (2001), as the flare may be due to jet emission (Markoff et al. 2001). Besides the flare period, the quiescent Sgr A\* deviates from the fundamental plane (Falcke et al. 2004; K rding et al. 2006). Recent study shows that the mass of M82 X-1 is  $428 \pm 105 M_{\odot}$ , which belongs to an intermediate-mass BH (Pasham et al. 2014). We must note that the mass is determined by extrapolating the inverse-mass scaling that holds for stellar-mass black holes (Pasham et al. 2014), but whether this scaling can be extrapolated is unclear. The simultaneous observation shows that the X-ray luminosity is about  $2.4 \times 10^{40} \text{ erg s}^{-1}$  and radio luminosity is  $(6.7 \pm 1.3) \times 10^{40} \text{ erg s}^{-1}$  (Kaaret et al. 2006).

It must be noted that the XRBs in the low/hard state are not flaring, and the Sgr A\* is flaring in our sample. There are two states for XRBs: the high/soft state with a soft power-law spectrum dominated by a thermal ‘‘bump’’, and the low/hard state characterized by a dominant hard power-law and weak-to-absent thermal spectrum. On the other hand, some low-power AGN classes seem to lack evidence of a blue bump, and are analogous to the hard-state XRBs. These are FR I radio galaxies, BL Lacs and LINERs. The Sgr A\* may also be in this category. Interestingly, the flares in Sgr A\* (Baganoff et al. 2001) have a hard spectrum, so it may be analogous to the low/hard state in XRBs. Observations showed that XRBs produce powerful collimated outflows in the low/hard state (Fender 2001). The evidence of jet from Sgr A\* in flaring state also was found using high-resolution Very Large Array images and ultra-deep imaging-spectroscopic data from Chandra X-ray Observatory (Li et al. 2013). In quiescent state, independent evidences showed that a jet does not appear in Sgr A\* (Shen et al. 2005; Doeleman et al. 2008). So our sample contains the non-flaring XRBs in the low/hard state and the flaring Sgr A\*.

Although, the radiation in an advection-dominated accretion flow (ADAF) (Narayan & Yi 1994) is dominated by thermal Comptonization, in agreement with observations of XRBs in the low/hard state (Narayan 2005). For example, combining the thin disk model and the ADAF model, Narayan et al. (1996) and Esin et al. (1997) showed that the various spectral states of XRBs could be understood. The ADAF model or its variants (Blandford & Begelman 1999; Narayan et al.

2000), can explain many observations of XRBs (Esin et al. 1998, 2001). Meanwhile, as discussed above, the X-ray emission of the low/hard state XRBs can also be produced by a jet. When the X-ray luminosity is below a critical value ( $10^{-5}$  to  $10^{-6} L_{\text{edd}}$ ), the X-ray emission should be dominated by the emission from the jet (Yuan & Cui 2005). So in this paper, we assume that the X-ray emissions of low/hard state XRBs are mainly from jets.

The X-ray luminosity and radio luminosity used in fundamental plane should be taken quasi-simultaneously. But the simultaneous observations are rare. For AGNs, the radio and X-ray observations are usually non-simultaneous. Sometimes, there is more than a year between the different observations (Körding et al. 2006). But the orientation of this uncertainty is likely to be isotropic (Körding et al. 2006). Bell et al. (2011) showed that the time-lag between the X-ray and radio bands is about 40 days for NGC 7213. Interestingly, NGC 7213 lies very close to the best-fitting correlation of the fundamental plane. Miller et al. (2010) proposed that an individual source might not be rigidly governed by the fundamental plane on short timescales. But it follows the fundamental plane in a time-averaged sense. Although the emission regions producing the radio and the X-ray emission may be different. For GRBs, because of lacking the radio emission in the prompt phase, we use the peak luminosities of X-ray and radio bands, which is similar to the average radio and X-ray luminosities for AGNs. Meanwhile, the time lags between X-ray and radio observations for GRBs are from 1 day to 50 days (Chandra & Frail 2012). So the time lags is comparable to that of AGNs.

### 3 RESULTS

The fundamental plane reads

$$\log L_X = a_R \log L_R + a_M \log M + b, \quad (4)$$

where  $L_X$  is the X-ray luminosity,  $L_R$  is the radio luminosity at 5 GHz,  $M$  is the mass of BH, and  $a_R$ ,  $a_M$  and  $b$  are fitting parameters. In order to derive the best-fitting parameters for three variables with errors, we use the merit function (Press et al. 1992; Merloni et al. 2003; Körding et al. 2006), which is defined as:

$$\hat{\chi}^2 = \sum_i \frac{(y_i - b - \sum_j a_j x_{ij})^2}{\sigma_{y_i}^2 + \sum_j (a_j \sigma_{x_{ij}})^2}, \quad (5)$$

where  $y_i$  denotes the X-ray luminosity,  $x_{1j}$  is the radio luminosity,  $x_{2j}$  is the mass of BH, and  $\sigma$  are the corresponding uncertainties. Because the standard  $\chi^2$  fit only considers the scatter of variable in the  $y$ -axis. This merit function includes all the errors of parameters.

Figure 1 shows the fundamental plane of BH activity including the XRBs and AGNs from K rding et al. (2006), the intermediate-mass BH M82 X-1, and GRBs. In this figure, the mass of BH for GRB is fixed to be  $3M_{\odot}$ . The value of y axis is  $\log L'_X = \log L_X - a_M \log M$ . Using the merit function, we derive the best-fitting results for the sample of K rding et al. (2006) are  $a_R = 1.41 \pm 0.12$ ,  $a_M = -0.87 \pm 0.17$ , and  $b = -4.90 \pm 3.35$ . While for the GRB sample, the parameters are  $a_R = 1.38 \pm 0.17$ ,  $a_M = -0.87 \pm 0.20$ , and  $b = -5.02 \pm 3.20$ . The solid blue line is the best fit of the combined sample. The parameters are  $a_R = 1.40 \pm 0.18$ ,  $a_M = -0.89 \pm 0.22$ , and  $b = -5.0 \pm 3.40$ . The fitted result of the jet-dominated model is  $a_R = 1.38$ ,  $a_M = -0.81$  (Falcke et al. 2004), while the fitted result of disk-jet model is  $a_R = 1.64$ , and  $a_M = -1.3$  (Merloni et al. 2003). Our results are dramatically consistent with the jet-dominated model. Interestingly, the M82 X-1 with about  $400M_{\odot}$  also follows this correlation. Figure 2 presents the fundamental plane of black hole activities same as Figure 1, except that the mass of BH for GRB is assumed as  $10M_{\odot}$ . The fitting parameters of GRBs are  $a_R = 1.41 \pm 0.15$ ,  $a_M = -0.89 \pm 0.20$ , and  $b = -5.50 \pm 3.60$ , which is shown as the black line. The blue line shows the best fit of the whole sample. The intermediate-mass BH M82 X-1 also follows this correlation.

The X-ray and radio emission of GRBs is highly beamed (Rhoads 1997). So the intrinsic luminosity should be calculated by  $L = L_{\text{iso}} F_{\text{beam}} = L_{\text{iso}}(1 - \cos \theta_j)$ , where  $L_{\text{iso}}$  is the isotropic luminosity and  $\theta_j$  is the jet opening angle. For AGNs,  $F_{\text{beam}} = 1 - \cos 1/\Gamma$ , where  $\Gamma$  is the bulk Lorentz factor of the outflow, because  $\theta_j < 1/\Gamma$  for AGNs. The jet opening angle  $\theta_j$  for GRBs can be derived from the break time of the afterglow light curve. We use the value of  $\theta_j$  from Wang et al. (2011) and Wang et al. (2014). For AGNs, the Lorentz factor and viewing angle can be estimated from their variable brightness and apparent jet speed (Ghisellini et al. 1993). Because of lack of observations, it's very hard to derive all the Lorentz factor of AGNs. Moreover, if the X-rays originate from the disk or corona, they will not be beamed. For jet models, the X-ray emission may be beamed like the radio emission or have a different beaming patterns. So we can only assume isotropy (K rding et al. 2006). In Figure 3, we show the fundamental plane of BH activity after correcting the beaming factor of GRBs. The masses of GRBs are assumed as  $3M_{\odot}$ . The fitting result of GRBs is shown as the black line with parameters,  $a_R = 1.375 \pm 0.19$ ,  $a_M = -0.88 \pm 0.22$  and  $b = -4.35 \pm 3.10$ . These results are consistent with that of XRBs, M82 X-1 and AGNs. This consistence can be expected. As in the jet-dominated model, the X-ray and radio luminosities are both corrected by a factor of  $(1 - \cos \theta_j)$ . By considering the relativistic beaming, Plotkin et al. (2012) found that relativistically beamed BL Lac objects fit well onto the fundamental plane. The slopes of the fundamental plane are almost unchanged when the beaming

effect is included (Plotkin et al. 2012). The fundamental plane is weakly dependent on the beaming factor (Körding et al. 2006).

#### 4 SUMMARY

In this paper, we have found that a correlation exists between the radio luminosity, X-ray luminosity, and BH mass among stellar-mass, intermediate-mass, and supermassive BHs, which is called the fundamental plane of BH activity. The analogy known to exist between XRBs in the low/hard state and AGNs can be extended to GRBs and intermediate-mass BH M82 X-1. Our results suggest that the underlying physics of the fundamental plane is that the X-ray and radio emission is produced by a jet, which is called the jet-dominated model. The jets are scale-invariant with respect to the BH mass. So it is possible to use the fundamental plane to estimate BH masses, especially for the intermediate-mass BHs and GRBs.

#### ACKNOWLEDGEMENTS

We thank the anonymous referee for constructive comments. We thank F. Yuan, Y. C. Zou and B. Zhang for helpful discussions. This work is supported by the National Basic Research Program of China (973 Program, grant No. 2014CB845800) and the National Natural Science Foundation of China (grants 11422325, 11373022, and 11573014), and the Excellent Youth Foundation of Jiangsu Province (BK20140016).

#### REFERENCES

- Baganoff, F. K., Bautz, M. W., Brandt, W. N., et al. 2001, *Nature*, 413, 45
- Band, D. et al. 1993, *ApJ*, 413, 281
- Bell, M. E. et al. 2011, *MNRAS*, 411, 402
- Blandford, R. D. & Begelman, M. C., 1999, *MNRAS*, 303, L1
- Butler, N. B. et al. 2007, *ApJ*, 671, 656
- Butler, N. B., et al. 2010, *ApJ*, 711, 495
- Chandra, P. & Frail, D. A. 2012, *ApJ*, 746, 156
- Corbel, S., Fender, R. P., Tzioumis, A. K., Nowak, M., McIntyre, V., Durouchoux, P. & Sood, R. 2000, *A&A*, 359, 251
- Corbel S., Fender R. P., Tomsick J. A., Tzioumis A. K., Tingay S., 2004, *ApJ*, 617, 1272



- Coriat, M., Corbel, S., Prat L., et al. 2011, MNRAS, 414, 677
- Dessart, L., Connor, E. & Ott, C. D. 2012, ApJ, 754, 76
- Doeleman, S. S., Weintroub, J., Rogers, A. E. E., et al. 2008, Natur, 455, 78
- Dong, A., Wu, Q. W. & Cao, X. F. 2014, ApJL, 787, L20
- Eichler, D., Livio, M., Piran, T., & Schramm, D. N. 1989, Nature, 340, 126
- Esin, A. A., McClintock, J. E., Drake, J. J., Garcia, M. R., Haswell, C. A., Hynes, R. I. & Munro, M. P., 2001, ApJ, 555, 483
- Esin, A. A., McClintock, J. E. & Narayan, R., 1997, ApJ, 489, 865.
- Esin, A. A., Narayan, R., Cui, W., Grove, J. E. & Zhang, S.-N.: 1998, ApJ, 505, 854
- Falcke, H., Körding, E. & Markoff, S. 2004, A&A, 414, 895
- Farrell, S. A. et al. 2009, Nature, 460, 73
- Fender R. P., 2001, MNRAS, 322, 31
- Gallo, E., Fender, R. P. & Pooley, G. G. 2003, MNRAS, 344, 60
- Gehrels, N., Ramirez-Ruiz, E. & Fox, D. B. 2009, ARA&A, 47, 567
- Ghisellini, G., Padovani, P., Celotti, A. & Maraschi, L. 1993, ApJ, 407, 65
- Golenetskii, S. et al. 2007, GRB Coordinates Network Circular, 6049, 1
- Golenetskii, S. et al. 2009a, GRB Coordinates Network Circular, 9030, 1
- Golenetskii, S. et al. 2009b, GRB Coordinates Network Circular, 9050, 1
- Gültekin, K., Cackett, E. M., King, A. L., Miller, J. M. & Pinkney, J. 2014, ApJ, 788, L22
- Heinz, S. & Sunyaev, R. A. 2003, MNRAS, 343, 59
- Ho, L. C. 2005, Astrophys. Space Sci., 300, 219
- Homan, J., Buxton, M., Markoff, S., et al. 2005, ApJ, 624, 295
- Jonker, P. G., Miller-Jones, J., & Homan, J. 2010, MNRAS, 401, 1255
- Kaaret, P., Simet, M. G. & Lang, C. C. 2006, ApJ, 646, 174
- Körding, E. 2014, Space Sci. Rev., 183, 149
- Körding, E., Falcke, H. & Corbel, S. 2006, A&A, 456, 439
- Kumar P. & Zhang B., 2015, Physics Reports, 561, 1
- Li, Z., Wu, X. B. & Wang, R. 2008, ApJ, 688, 826
- Li, Z. Y., Morris, M. R. & Baganoff, F. K. 2013, ApJ, 779, 2
- Lü, J. et al. 2015, RAA, 15, 617
- Lyu, F. et al. 2014, ApJ, 793, 36
- MacFadyen, A. I. & Woosley, S. E. 1999, ApJ, 524, 262
- Markoff, S., Falcke, H., Yuan, F., & Biermann, P. L. 2001, A&A, 379, L13

- Markoff, S., Nowak, M., Corbel, S., Fender, R. & Falcke, H. 2003, *A&A*, 397, 645
- Markoff, S., & Nowak, M. A. 2004, *ApJ*, 609, 972
- Markoff, S., Nowak, M. A., & Wilms, J. 2005, *ApJ*, 635, 1203
- McHardy, I. M., Köding, E., Knigge, C., Uttley, P. & Fender, R. P. 2006, *Nature*, 444, 739
- Meier, D. L. 2003, *New Astron. Rev.*, 47, 667
- Miller, J. M. et al., 2010, *ApJ*, 720, 1033
- Merloni, A., Heinz, S. & Di Matteo, T. 2003, *MNRAS*, 345, 1057
- Mészáros, P. 2006, *Rep. Prog. Phys.*, 69, 2259
- Merloni, A., Köding, E., Heinz, S., Markoff, S., Di Matteo, T. & Falcke, H. 2006, *New Astron.*, 11, 567
- Mirabel, I. F. & Rodriguez, L. F. 1999, *ARA&A*, 37, 409
- Nakar, E. 2007, *Phys. Rep.*, 442, 166
- Narayan, R., Igumenshchev, I. V. & Abramowicz, M. A., 2000, *ApJ*, 539, 798
- Narayan, R. 2005, *Astrophys. Space Sci.*, 300, 177
- Narayan, R. & Yi, I., 1994, *ApJ*, 428, L13
- Narayan, R., McClintock, J. E. & Yi, I., 1996, *ApJ*, 457, 821
- Nava, L. et al. 2012, *MNRAS*, 421, 1256
- Nemmen, R. S. et al. 2012, *Science*, 338, 1445
- Pasham, D. R., Strohmayer, T. E. & Mushotzky, R. F. 2014, *Nature*, 513, 74
- Piran, T. 2004, *Rev. Mod. Phys.*, 76, 1143
- Plotkin, R. M., Markoff, S., Kelly, B. C., Körding, E. & Anderson, S. F. 2012, *MNRAS*, 419, 267
- Poutanen J., 1998, in Abramowicz M. A., Björnsson G., Pringle J. E., eds, *Theory of Black Hole Accretion Discs*, Cambridge Contemporary Astrophysics. Cambridge Univ. Press, Cambridge, p. 100
- Press, W. H., Teukolsky, S. A., Vetterling, W. T. & Flannery, B. P. 1992, *Numerical Recipes*, 2nd edn. Cambridge Univ. Press, Cambridge
- Ratti, E. M., Jonker, P. G., Miller-Jones, J. A. C., et al. 2012, *MNRAS*, 423, 2656
- Remillard, R. A. & McClintock, J. E. 2006, *ARA&A*, 44, 49
- Rees, M. J. & Mészáros, P., 1994, *ApJ*, 430, L93
- Rhoads, J. E. 1997, *ApJ*, 487, L1
- Sari, R., Piran, T. & Narayan, R. 1998, *ApJ*, 497, L17
- Schaefer, B. E. 2007, *ApJ*, 660, 16
- Shen, Z.-Q., Lo, K. Y., Liang, M.-C., Ho, P. T. P., & Zhao, J.-H. 2005, *Natur*, 438, 62

- Wang, F. Y., Qi, S. & Dai, Z. G. 2011, MNRAS, 415, 3423
- Wang, F. Y., Yi, S. X. & Dai, Z. G. 2014, ApJ, 786, L8
- Wang, F. Y., Dai, Z. G., & Liang, E. W. 2015, NewAR, 67, 1
- Wang, F. Y., Dai, Z. G., Yi, S. X. & Xi, S. Q. 2015, ApJS, 216, 8
- White, N. E., Fabian, A. C. & Mushotzky, R. F. 1984, A&A, 133, 9
- Woosley, S. E. 1993, ApJ, 405, 273
- Wu, Q. et al. 2016, MNRAS, 455, L1
- Xie, F. & Yuan, F. 2017, ApJ, 836, 1
- Younes, G., et al., 2012, A&A, 539, 104
- Yuan, F. & Cui, W. 2005, ApJ, 629, 408
- Yuan, F., Yu, Z. & Ho, L. C. 2009, ApJ, 703, 1034
- Zhang, B. & Mészáros, P. 2004, IJMPA, 19, 2385

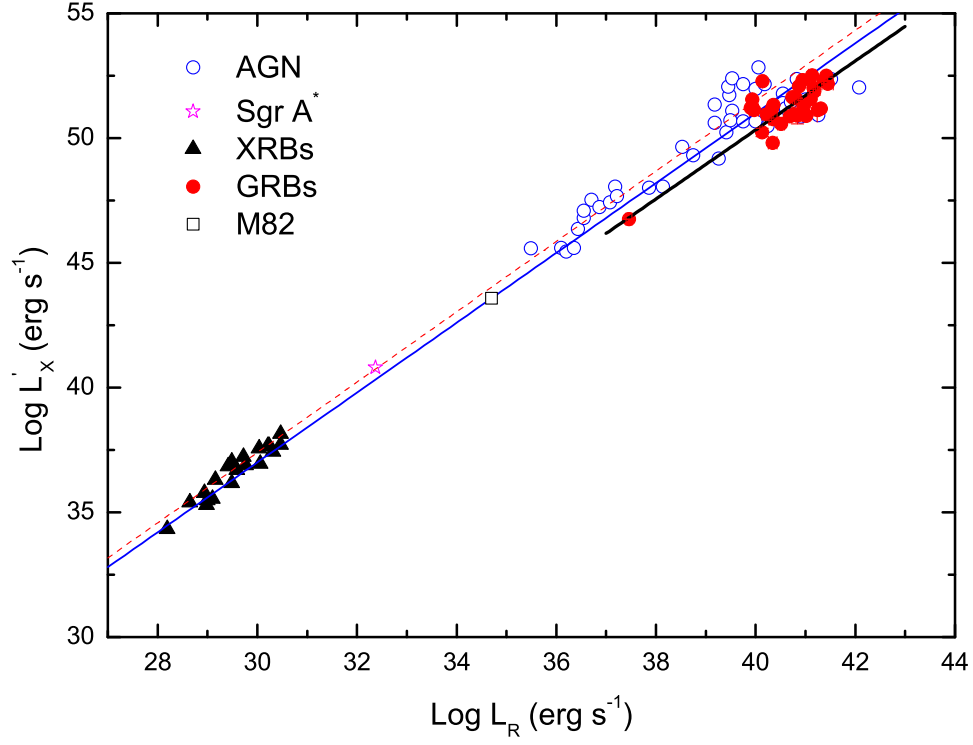


**Figure 1.** The fundamental plane of BH activity. The mass of BH for GRB is assumed to be  $3M_{\odot}$ . The black line represents the best fitting of GRBs. The red line is the best fitting for the XRBs and AGNs, and the blue line is the best fitting for the whole sample ( $\log L_X = (1.41 \pm 0.12) \log L_R - (0.87 \pm 0.17) \log M - (4.90 \pm 3.35)$ ). The square is M82 X-1, which is dramatically consistent with the best fitting. So the universal scaling law of BH activity exists in stellar-mass, intermediate and supermassive BHs.

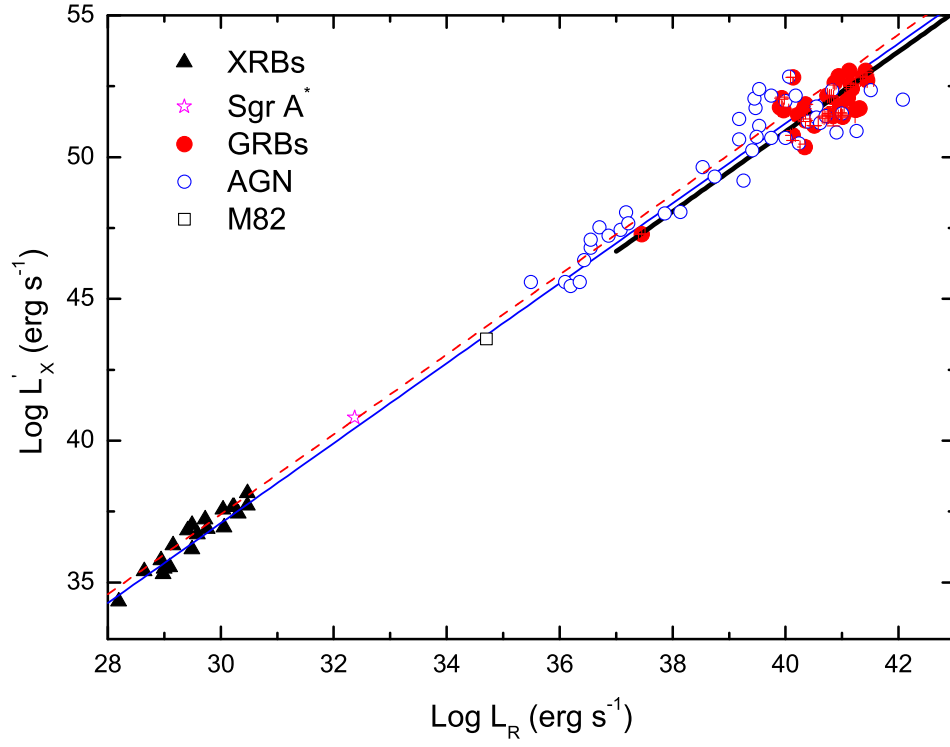


**Figure 2.** The same as Figure 1, except that the masses of GRB BHs are fixed as  $10M_{\odot}$ . The best fitting results for the whole sample is  $\log L_X = (1.41 \pm 0.20) \log L_R - (0.88 \pm 0.18) \log M - (5.21 \pm 3.50)$ .

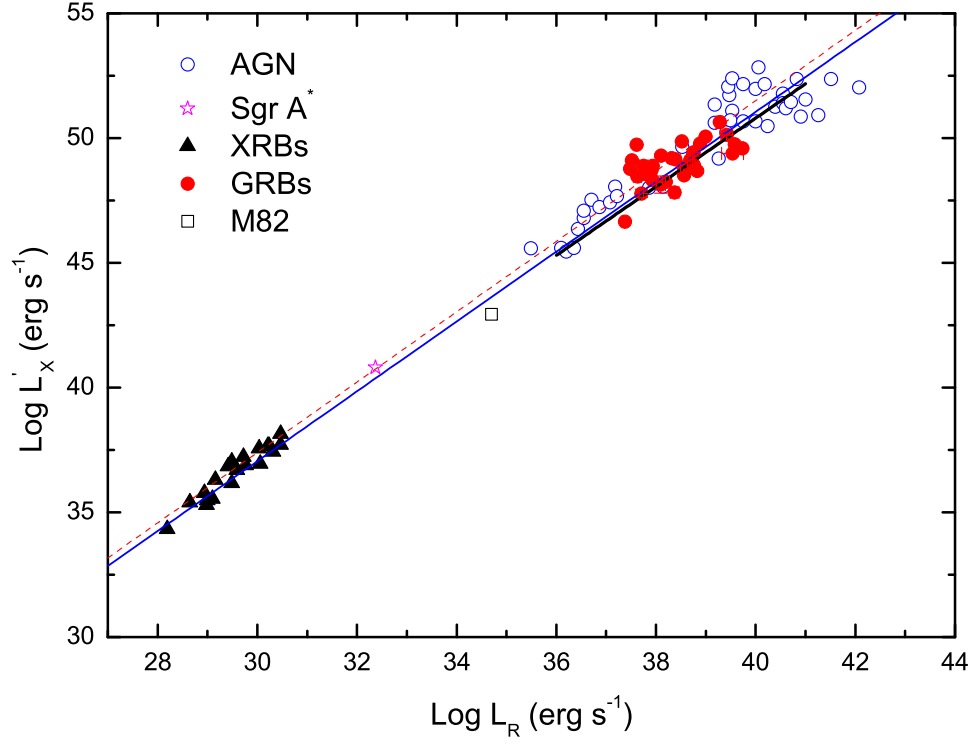


**Figure 3.** The fundamental plane of BH activity. The black line represents the best fitting of GRBs with beaming corrected. The mass of BH for GRB is assumed to be  $3M_{\odot}$ . The red line is the best fitting for the XRBs and AGNs from K rding et al. (2006), and the blue line is the best fitting for the whole sample. The square represents the M82 X-1, which is dramatically consistent with the best fitting. So the universal scaling law of BH activity is not affected by the beaming effect.

GRB	$z$	$P^a$	$E_{peak}$ keV	$E_{min}$ keV	$E_{max}$ keV	$\alpha$	$\beta$	$F_R$ $\mu\text{Jy}$	Frequency GHz	Ref <sup>b</sup>
970508	0.835	7.4E-7 $\pm$ 7E-8	389 $\pm$ 40	40	700	-1.19 $\pm$ 0.1	-1.83 $\pm$ 0.4	780 $\pm$ 13	4.86	1,2
970828	0.958	3.0E-6 $\pm$ 3E-7	298 $\pm$ 30	50	300	-0.7 $\pm$ 0.1	-2.07 $\pm$ 0.4	144 $\pm$ 31	8.46	1,2
980703	0.966	2.4 $\pm$ 0.06	254 $\pm$ 25	50	300	-1.31 $\pm$ 0.1	-2.4 $\pm$ 0.4	1055 $\pm$ 30	4.86	1,2
990510	1.619	8.17 $\pm$ 0.08	126 $\pm$ 10	50	300	-1.28 $\pm$ 0.1	-2.67 $\pm$ 0.4	255 $\pm$ 34	8.46	1,2
010222	1.477	8.6E-6 $\pm$ 2E-7	309 $\pm$ 12	40	700	-1.35 $\pm$ 0.19	-1.64 $\pm$ 0.02	93 $\pm$ 25	8.46	1,2
021004	2.33	0.89 $\pm$ 0.20	80 $\pm$ 38	30	400	-1.01 $\pm$ 0.18	-2.2 $\pm$ 0.4	470 $\pm$ 26	4.86	1,2
030226	1.986	0.99 $\pm$ 0.17	97 $\pm$ 17	30	400	-0.89 $\pm$ 0.16	-2.2 $\pm$ 0.4	171 $\pm$ 23	8.46	1,2
030329	0.169	72.2 $\pm$ 3.8	68 $\pm$ 2.2	30	400	-1.26 $\pm$ 0.02	-2.28 $\pm$ 0.06	10337 $\pm$ 33	4.86	1,2
050416A	0.65	4.8 $\pm$ 0.4	15 $\pm$ 2.7	15	350	-1.1 $\pm$ 0.4	-3.4 $\pm$ 0.4	485 $\pm$ 36	4.86	1,2
050603	2.821	31.8 $\pm$ 1.7	344 $\pm$ 52	15	350	-1.03 $\pm$ 0.06	-2.03 $\pm$ 0.1	377 $\pm$ 53	8.46	1,2
050820A	2.615	1.3 $\pm$ 0.2	246 $\pm$ 40	15	150	-1.25 $\pm$ 0.10	-2.2 $\pm$ 0.4	150 $\pm$ 31	8.46	1,2
050904	6.29	0.8 $\pm$ 0.1	436 $\pm$ 90	15	150	-1.11 $\pm$ 0.06	-2.2 $\pm$ 0.4	76 $\pm$ 14	8.46	1,2
051022	0.809	1.0E-5 $\pm$ 8E-7	510 $\pm$ 20	20	2000	-1.176 $\pm$ 0.02	-2.2 $\pm$ 0.4	268 $\pm$ 32	8.46	1,2
060218	0.033	0.021 $\pm$ 0.005	4.9 $\pm$ 0.3	15	150	-0.84 $\pm$ 0.1	-2.2 $\pm$ 0.4	245 $\pm$ 50	4.86	2,3
070125	1.548	2.25E-5 $\pm$ 3.4E-6	367 $\pm$ 51	20	10000	-1.1 $\pm$ 0.1	-2.08 $\pm$ 0.15	1028 $\pm$ 16	8.46	2,4
071003	1.604	1.11E-6 $\pm$ 1.0E-7	799 $\pm$ 100	15	350	-1.31 $\pm$ 0.07	-2.2 $\pm$ 0.4	616 $\pm$ 57	8.46	2,3
071010B	0.947	5.48E-7 $\pm$ 5E-8	52 $\pm$ 6	15	150	-1.5 $\pm$ 0.2	-2.2 $\pm$ 0.4	227 $\pm$ 114	4.86	2,5
090323	3.57	5.96E-6 $\pm$ 1.06E-6	416 $\pm$ 76	20	10000	-0.96 $\pm$ 0.09	-2.09 $\pm$ 0.22	243 $\pm$ 13	8.46	2,6
090328	0.736	12.2E-5 $\pm$ 2.5E-6	592 $\pm$ 237	20	8000	-1.04 $\pm$ 0.1	-2.05 $\pm$ 0.9	686 $\pm$ 26	8.46	2,7
090423	8.26	1.02E-7 $\pm$ 8E-8	49 $\pm$ 3.8	15	150	-0.77 $\pm$ 0.08	-2.2 $\pm$ 0.4	50 $\pm$ 11	8.46	2,5,8
090424	0.544	9.12E-6 $\pm$ 1.4E-7	162 $\pm$ 3.4	8	35000	-1.02 $\pm$ 0.01	-3.26 $\pm$ 0.14	236 $\pm$ 37	8.46	2,9
090715B	3	9E-7 $\pm$ 9E-8	134 $\pm$ 40	20	2000	-1.1 $\pm$ 0.37	-2.2 $\pm$ 0.4	191 $\pm$ 36	8.46	2,9
091020	1.71	1.88E-6 $\pm$ 2.6E-7	187 $\pm$ 34	8	35000	-1.2 $\pm$ 0.06	-2.29 $\pm$ 0.18	399 $\pm$ 21	8.46	2,9
100418A	0.62	6.62E-8 $\pm$ 3.6E-8	25 $\pm$ 3.0	15	150	-1.0 $\pm$ 0.1	-2.06 $\pm$ 0.3	522 $\pm$ 83	4.86	2,10
100814A	1.44	7.5E-7 $\pm$ 2.5E-7	128 $\pm$ 23	20	2000	-1.1 $\pm$ 0.2	-2.2 $\pm$ 0.4	496 $\pm$ 24	4.5	1
991216	1.02	67.52 $\pm$ 0.23	318 $\pm$ 30	50	300	-1.23 $\pm$ 0.1	-2.18 $\pm$ 0.4	126	4.86	1,2
000210	0.85	29.9 $\pm$ 3.0	408 $\pm$ 14	50	300	-1.1 $\pm$ 0.4	-2.2 $\pm$ 0.4	93	8.46	1,2
050401	2.898	12.6 $\pm$ 1	118 $\pm$ 18	20	2000	-0.9 $\pm$ 0.3	-2.55 $\pm$ 0.3	122	8.46	1,2
050525A	0.606	48.0 $\pm$ 0.6	81.2 $\pm$ 1.4	15	350	-1.01 $\pm$ 0.06	-3.26 $\pm$ 0.2	164	8.46	1,2
050824	0.83	0.5 $\pm$ 0.2	15 $\pm$ 2	15	150	-1.1 $\pm$ 0.4	-3.3 $\pm$ 1.0	152	8.46	1,2
060418	1.49	6.7 $\pm$ 0.2	230 $\pm$ 20	15	150	-1.5 $\pm$ 0.1	-2.2 $\pm$ 0.4	216	8.46	1,2
071020	2.146	6.04E-6 $\pm$ 2.08E-6	322 $\pm$ 65	20	2000	-0.65 $\pm$ 0.29	-2.0 $\pm$ 0.4	141	8.46	2,9

**Table 1.** GRB data.<sup>a</sup>The reported  $P$  value is either in units of photons  $\text{cm}^{-2} \text{s}^{-1}$  for values larger than 0.01 (not in scientific notation) or in units of  $\text{erg cm}^{-2} \text{s}^{-1}$  for values smaller than 0.01 (those in scientific notation). <sup>b</sup>(1) Schaefer (2007); (2) Chandra & Frail (2012); (3) Butler et al. (2007); (4) Golenetskii et al. (2007); (5) Butler et al. (2010); (6) Golenetskii et al. (2009a); (7) Golenetskii et al. (2009b); (8) Wang et al. (2011); (9) Nava et al. (2012); (10) <http://butler.lab.asu.edu/swift>.